






Article

Hydrophobic and Photocatalytic Treatment for the Conservation of Painted *Lecce stone* in Outdoor Conditions: A New Cleaning Approach

Laura Bergamonti ^{1,*} , Marianna Potenza ¹ , Federica Scigliuzzo ¹, Sandro Meli ¹, Antonella Casoli ¹ , Pier Paolo Lottici ²  and Claudia Graiff ^{1,*} 

¹ Department of Chemistry, Life Sciences and Environmental Sustainability, University of Parma, Parco Area delle Scienze 17a, 43124 Parma, Italy; marianna.potenza@unipr.it (M.P.); federica.scigliuzzo@gmail.com (F.S.); sandro.meli@unipr.it (S.M.); antonella.casoli@unipr.it (A.C.)

² Department of Mathematical, Physical and Computer Sciences, University of Parma, Parco Area delle Scienze 7a, 43124 Parma, Italy; pierpaolo.lottici@unipr.it

* Correspondence: laura.bergamonti@unipr.it (L.B.); claudia.graiff@unipr.it (C.G.)

Featured Application: TiO₂/OrMoSil-based coatings can be employed as an effective cleaning method to preserve painted carbonate stones. The treatment is also efficient as a protective coating to slow down the degradation phenomena.

Abstract: Self-cleaning and hydrophobic treatments based on TiO₂ and SiO₂ nanoparticles are widely applied for the preservation of cultural heritage materials, to improve their resilience in polluted environments. Excellent results have been obtained on stone materials, but experiments on painted stone surfaces, such as wall paintings and polychrome plasters used in historic buildings, are still limited. In this work, we present a study on the use of water dispersions of TiO₂ nanoparticles obtained via sol-gel and organically modified silica (OrMoSil) for cleaning and protective purposes on *Lecce stone*, a carbonate stone, widely used for its excellent workability but easily attacked by atmospheric agents and pollutants. First, we evaluated the harmlessness of the treatment on *Lecce stone* through colorimetric tests, water absorption by capillarity and permeability to water vapor. The photocatalytic activity of the TiO₂ nanoparticles was assessed by photo-degradation of methyl orange and methylene blue dyes. The dispersion was then applied on painted samples prepared according to ancient recipes to confirm the effectiveness of the cleaning. The proposed TiO₂/OrMoSil-based coating can act as a self-cleaning and protective treatment on lithic surfaces to prevent degradation phenomena and preserve the original appearance of the monument.

Keywords: painted stone cleaning; self-cleaning and hydrophobic coating; photocatalysis; TiO₂; OrMoSil



Citation: Bergamonti, L.; Potenza, M.; Scigliuzzo, F.; Meli, S.; Casoli, A.; Lottici, P.P.; Graiff, C. Hydrophobic and Photocatalytic Treatment for the Conservation of Painted *Lecce stone* in Outdoor Conditions: A New Cleaning Approach. *Appl. Sci.* **2024**, *14*, 1261. <https://doi.org/10.3390/app14031261>

Academic Editor: Ion Sandu

Received: 9 January 2024

Revised: 27 January 2024

Accepted: 30 January 2024

Published: 2 February 2024



Copyright: © 2024 by the authors. Licensee MDPI, Basel, Switzerland. This article is an open access article distributed under the terms and conditions of the Creative Commons Attribution (CC BY) license (<https://creativecommons.org/licenses/by/4.0/>).

1. Introduction

The application of painted layers on lithic materials, in both architectural and sculptural fields, was a very common practice in ancient cultures such as the Egyptian, Greek and Roman ones but also in the Romanesque, Gothic and Baroque periods up to modern and contemporary works [1–5]. Nowadays, traces of the original pictorial layers on the outdoor architectural works of art are rather rare, partly due to natural ageing caused by atmospheric agents (water, climate and pollution) and partly because over the centuries, there have been many interventions on the architecture or even just on the coloring of the buildings, adapting them to new styles. Starting from the middle of the 19th century, the “Purist current” interventions had an even more deleterious effect, because, aiming at radical cleaning, they inexorably led to the elimination of both the plasterworks, including the original ones, and many decorations [2].

Every conservation and restoration intervention used on cultural heritage must aim to preserve the original appearance of the work of art and the integrity of the support material [6–9]. However, painted lithic surfaces, exposed to the outdoors, require frequent conservative treatments due to solar radiation and hostile weather conditions, atmospheric pollution, vandalism and accidental damage [4,10,11]. These agents can accelerate stone decay and produce aesthetically unacceptable stains on stone surfaces [12–15]. Although the removal of dirty material is necessary to slow down the decay processes and preserve the aesthetic quality of buildings, it should be underlined that cleaning intervention is an invasive and irreversible operation, and the use of chemicals reagents could lead to alteration of the aesthetic appearance and the release of by-products that can damage works of art and the environment [16–20].

There are basically two essential problems related to this intervention of conservative restoration: the first one is to establish what should be removed and the second is related to the choice of the method [6,21]. As reported in the dedicated literature, the cleaning of a lithic monument should meet some requirements [6,22,23]: no damage can be caused to the substrate such as fracturing, abrasion, dissolution of the material; variation of the porosity; and, obviously, color change. This is crucial when the surface of the monument to be cleaned has a painted layer on it.

In addition, the performance of the cleaning method must be evaluated by means of laboratory testing trials. In general, the choice of the appropriate cleaning method must be made after a careful analysis of the surface to be treated, considering the type of stone, the type of pictorial layer, their physical and chemical characteristics and the extent and severity of the decay alteration [24–28].

Finally, to limit further invasive cleaning interventions, it is necessary to implement preventive measures and lasting actions, such as the application of hydrophobic and self-cleaning treatments. In fact, an important requirement for protective treatments for buildings is to protect against water, which is the main vehicle for the various degradation agents of the porous structure of building material [29–32].

Several cleaning procedures (chemical, mechanical, laser, and biological methods) have been proposed [10,33–37]. Among these, chemical and mechanical methods are the most used by restorers. Chemical cleaning is based on the reaction between an applied solvent and the material to be removed, achieving its dissolution and extraction [22]. The chemicals used are typically organic solvents or alkali caustic removers, not always healthy for the restorer and the environment [38–40]. Mechanical cleaning involves an abrasive process of the surface, which can cause numerous forms of damage to the substrate and includes the risk of removing part of the original material [10].

Great interest has been directed in recent years towards the study and use of mini-invasive, efficient and environmentally friendly methods for cleaning surfaces [41–46]. Among the innovative cleaning methods of architectural elements, the use of photocatalysis has been largely investigated [47–54], with the most used photocatalyst being based on titanium oxide (TiO_2). In a heterogeneous photocatalysis system, the photoinduced transformations occur on the surface of the photocatalyst when light of appropriate wavelengths is absorbed (for example, TiO_2 in the anatase form has a band gap of about 3.2 eV, corresponding to $\lambda_{\text{max}} \approx 388 \text{ nm}$) with the production of electron-hole pairs. The generated electrons and holes migrate on the surface of the photocatalyst, where, together with reactive oxygen species produced via redox reactions, they can decompose several organic compounds [55,56]. Titanium dioxide, present in nature in three polymorphs, rutile, anatase and brookite, is one of the most studied photocatalysts because of its easy availability, high reactivity and chemical stability: it has been used in several applications, such as for the purification of environmental pollutants, for the decontamination of water and for its self-cleaning properties in the conservation of cultural heritage [57–63]. In recent years, numerous photocatalytic materials associated with superhydrophobic surface coatings have been developed for protecting exposed buildings and monuments. Superhydrophobic

materials can significantly limit damage due to water adsorption and contribute to the cleaning of the stone surfaces, restoring the aesthetic qualities of the artwork [30–32,64–66].

In this work, we present a preliminary investigation on the possibility of using photocatalysis on painted stone for cleaning purposes. Firstly, the harmlessness and effectiveness of a self-cleaning and protective treatment based on TiO₂ and OrMoSil on a carbonate stone (*Lecce stone*) were evaluated. TiO₂, used as a photocatalytic agent, was synthesized via sol-gel, as reported in [63], and its photocatalytic efficiency was compared with the well-known titanium dioxide P25 (Evonik, Essen, Germany), a mixture of nanocrystalline anatase and rutile. The OrMoSil hydrophobic coating was prepared by modifying the procedure described in [32]. The *Lecce stone* is typical of the Salento area, in the southeastern end of Italy, and was widely used during the Baroque period for the construction of civil and religious monuments and for the creation of sculptural works of art. It is characterized by a white-cream color, high porosity and excellent workability. *Lecce stone* consists predominantly of calcium carbonate (93–97%). From a petrographic point of view, it is a homogeneous planktonic foraminiferal biomicrite [67]. In the Salento area, there are some examples of painted *Lecce stone*. Of particular importance are the votive aedicule dedicated to Santa Maria Maddalena, entirely stuccoed and decorated, located in Nardò, which has recently been restored [68]; the Abbey of Santa Maria di Cerrate (Squinzano, Lecce, Italy), located in the monastic complex founded by the monks of the “Rule of Saint Basil” in the 12th century [69]; and the Basilica of Santa Caterina d’Alessandria in Galatina (Lecce, Italy), built between 1369 and 1391 [70].

The first part of the experiments was performed on raw *Lecce stone*, on which we evaluated the harmlessness of the TiO₂/OrMoSil treatment through colorimetric tests, measurements of water absorption through capillarity and of permeability to water vapor and its durability by means of artificial ageing and salt crystallization. Then we tested, with colorimetric methods, the self-cleaning efficacy of the coating in the photodegradation of methyl orange (MeO) and methylene blue (MB) dyes, commonly used as model pollutants, under artificial solar irradiation [71–74].

The second part of the experiments was carried out on samples of painted stone prepared according to ancient recipes using red ochre, one of the most used pigments by wall painters [75,76]. Firstly, through measurements of the color changes, it was verified that the TiO₂/OrMoSil treatment applied on the painted stone does not alter the original appearance of the colors. Then, on the painted specimens, the capability of the TiO₂/OrMoSil treatment to remove soiling and to provide preventive hydrophobic and self-cleaning properties was tested.

All tests were assessed according to the cultural heritage regulations established by the Italian Standardization Institute (UNI) and the European Standard (EN).

2. Materials and Methods

2.1. Lecce stone Samples: Petrographic Analysis

The petrographic analysis of the *Lecce stone* was carried out on thin sections (~30 μm) using a Nikon Eclipse E400 POL (Nikon Corporation, Minato-Ku, Tokyo, Japan) polarized optical microscope to evaluate the compositional and microstructural features (grain size, matrix, cement and porosity) under transmitted light.

2.2. Synthesis and Application of the Coatings

TiO₂ water-based sol (0.1 M), hereafter called N-TiA, was synthesized from titanium (IV) oxysulphate (TiOSO₄, Sigma-Aldrich, St. Louis, MO, USA) as a Ti precursor as reported in Fornasini [63]. Briefly, 1×10^{-2} mol of TiOSO₄, hydrolyzed in distilled water at 40 °C, were subjected to precipitation by slowly dripping ammonium hydroxide (NH₄OH, 26%, Carlo Erba, Milan, Italy) into the solution until the pH ≈ 7. The white precipitate was repeatedly washed with distilled water to eliminate the residual SO₄²⁻ ions (as checked by a BaCl₂ test). The resulting powder was suspended in distilled water (100 mL), followed by peptization with nitric acid (HNO₃ 65% Carlo Erba) until the pH was down to 1.3–1.5. The

suspension was left under vigorous stirring at room temperature for about 30 min until it became clear. The sol was then refluxed at 100 °C for 2 h to induce crystallization. The colorless final sol is slightly opalescent and does not show precipitates.

The organically modified silica coating (hereafter called TP-Hy) was prepared by using tetraethyl orthosilicate (TEOS, Sigma Aldrich) and hydroxyl-terminated polydimethylsiloxane (PDMS, Sigma Aldrich) as starting materials. Ethanol (EtOH, Sigma-Aldrich) and de-ionized water were used as solvents, while oxalic acid dihydrate (OxA, Sigma-Aldrich) was used as the catalyst [32]. The procedure was as follows: TEOS was hydrolyzed in a solution containing EtOH, H₂O and OxA in the molar ratio TEOS:EtOH:H₂O:OxA of 1:15:15:0.00015 under vigorous stirring at room temperature for 140 min. PDMS in a ratio of TEOS:PDMS = 1:0.1 (*v/v*) was then added to the previous solution and refluxed for 24 h.

The compatibility and effectiveness of the innovative self-cleaning surface treatment were preliminarily verified on samples of raw *Lecce stone*. Before the application of the coatings, 5 × 5 × 1 cm³ samples were dried at 60 °C in a ventilated oven for 24 h, kept 3 h in a dry atmosphere and then weighed. The procedure was repeated until constant weight was achieved according to UNI 10921:2001 [77]. Then the TP-Hy hydrophobic treatment was applied by brush directly on the stone samples, and three layers of N-TiA or of commercial P25 (for comparison) sols (0.1 M) were added. The P25 (pH ≈ 5) was applied as prepared, while N-TiA, before application, was repeatedly washed until a final pH ≈ 5 and re-suspended in distilled water [63]. The amounts of TP-Hy and TiO₂ coatings applied to the stone surface per unit area were held constant as accurately as possible. The stone samples were then stored in a desiccator at a temperature of 23 ± 1 °C.

2.3. Preparation of Painted *Lecce stone* Samples

The treatment was also tested on samples of painted *Lecce stone* (Figure 1). The painting mock-ups were prepared following the procedure described in the literature [78,79]. Red ochre powder, widely used in wall painting, was chosen as the pigment. It was dispersed in water and applied to a still wet layer of lime-based mortar. The samples thus prepared were dried in air for three weeks.

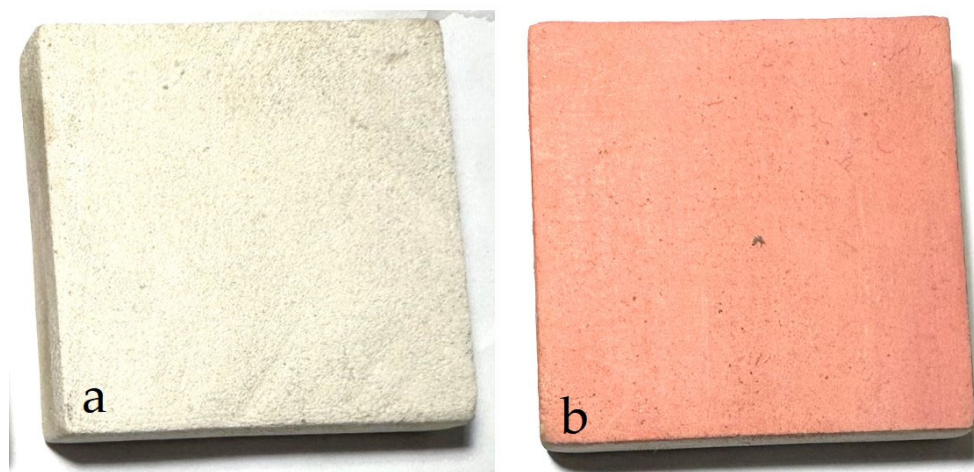


Figure 1. Raw (a) and painted (b) *Lecce stone* samples.

The painted samples were treated in two different modes for two types of tests:

- To assess the cleaning capacity of the treatment, the painted samples were preliminarily soiled with MB and MeO and subsequently coated with the TP-Hy/N-TiA or TP-Hy/P25 treatments. The test was done by measuring the disappearance of the stains under artificial solar radiation with the usual colorimetric methods.
- To evaluate the hydrophobic and self-cleaning properties, the TP-Hy/N-TiA or TP-Hy/P25 treatments were applied by brush directly on painted stones. Static contact

angle measurements were performed on the samples as prepared, and, subsequently, photocatalytic degradation of MB and MeO stains was assessed.

2.4. Characterization of the Applied Coatings

Raman measurements were carried out in a backscattered geometry with a LabRAM micro-spectrometer (Jobin Yvon Horiba, Kyoto, Japan) equipped with an Olympus BX40 microscope (Olympus Corporation, Tokyo, Japan). The 632.8 nm line of a 15 mW He–Ne laser was used, and the spectra were collected, at room temperature, by a long working distance $\times 50$ microscope objective lens.

XRD patterns were collected using a Thermo ARL X'TRA X-ray diffractometer equipped with Si–Li detector (Thermo Fisher Scientific Inc., Waltham, MA, USA). Cu–K α radiation (40 kV and 40 mA) at a 0.2° scan rate (in 2θ) in the range of 10–60° was used. Powdered silicon was used for 2θ calibration.

Morphological observations before and after the treatments and elemental analysis to study the distribution of the coatings on the raw stone surface were performed by means of a SEM-EDS system: a scanning electron microscope Jeol 6400 (Jeol Ltd.; Tokyo, Japan) equipped with an Oxford Instruments (Abingdon-on-Thames, UK) Analytical Link Si(Li) Energy Dispersive System Detector, with INCA V7.2 software.

The chromatic changes in the stone surface's appearance due to the TP-Hy and N-TiA treatments were evaluated according to UNI EN 15886:2010 rules [80] by colorimetric analysis performed by a Spectrodens colorimeter (Techkon GmbH, Königstein, Germany) on nine small zones. The results were averaged on three samples for each case. The color difference (ΔE^*) due to the coating was measured as

$$\Delta E^* = \sqrt{\Delta L^{*2} + \Delta a^{*2} + \Delta b^{*2}} \quad (1)$$

with ΔL^* being the change in lightness and Δa^* and Δb^* being the changes of the colorimetric coordinates a^* (red/green) and b^* (yellow/blue) in the CIELAB space.

The water absorption by capillarity was estimated on five samples before and after the treatments, according to UNI EN 15801:2010 [81]. The dried samples were placed on a Whatman multilayer paper (1 cm thick) saturated with deionized water. Samples were weighed at times $t_i = 10$ min, 20 min, 30 min, 60 min, 2 h, 4 h and 6 h and at following 24 h intervals until the difference between two successive weighings was $<1\%$ of the initial weight of the samples. The amount of absorbed water per unit area Q_i (kg/m²) was reported as a function of the square root of time ($t_i^{1/2}$), as, according to a well-known capillarity absorption model [82], there should be a linear relationship between the adsorbed water and the square root of time in short times. The value of the capillary water absorption coefficient AC (kg/(m² s^{1/2})) has been obtained from the slope of the linear fit in the first part (up to 60 min) of the capillarity graph (Q_i).

The water vapor permeability test was performed first on untreated stone and then after treatments, following the method proposed by Raneri et al. [16]: the $5 \times 5 \times 1$ cm³ samples were fixed on top of PVC containers, partially filled (one half) with water, and then the sealed containers were placed in a climatic chamber (RH 25% and $T = 25 \pm 0.5$ °C) and weighed every 24 h until constant vapor flow through the stone (i.e., the condition $((\Delta M_i - \Delta M_{i-1})/\Delta M_i) \times 100 \leq 5$ was reached). The vapor permeability reduction (VPR) was estimated as the mass of water vapor passing through the surface unit (cm²) in 24 h by $VPR\% = ((M_{uv} - M_{tv})/M_{uv}) \times 100$, where M_{uv} and M_{tv} are the mass of water vapor through the untreated and treated stone, respectively, measured at the steady state [83].

To evaluate the hydrophobic properties of the TP-Hy/N-TiA coating, static contact angle measurements were taken by the OCA25 OCA 25 device (DataPhysics Instruments, Filderstadt, Germany), using the sessile drop method, with 5 μ L drops applied via a needle to the stone surface before and after treatment, according to UNI 11207:2007 [84].

The artificial ageing test was performed on untreated and TP-Hy/N-TiA- and TP-Hy/P25-treated *Lecce stone* (three samples for each case). Four cycles of exposure

to rain and artificial solar radiation were made. Each 24 h cycle consists of 620 mm of water (i.e., the average annual rainfall in Salento) dropped on the samples, for 6 h, in the form of water mist, followed by 16 h of artificial solar irradiation under an Osram Ultra Vitalux lamp (300 W) (in UVA + B ~ 5.5 mW/cm² and in the 300–800 nm range ~ 56 mW/cm² [85]) and 2 h of dark at room conditions. The test was carried out in a closed container (45 × 35 × 30 cm³) equipped with a 45° inclined plane for housing the samples and with a lateral nebulization system with two nozzles. The hydrophobic properties of the coatings after ageing were tested by measuring the static contact angle at the end of each cycle.

Resistance to salt crystallization was assessed by adapting the procedure described in the standard UNI-EN 12370-2001 [86] on three *Lecce stone* samples (5 × 5 × 1 cm³) for each case. The samples, previously dried in an oven at 105 °C until a constant weight is reached, were weighed and then immersed in a 14% water solution of Na₂SO₄·10H₂O for 2 h at 20 °C. Then, the samples were dried in an oven at 105 °C for 16 h, cooled at room temperature in a desiccator for 2 h and weighed. The mass variation percentage with respect to the initial dry mass at the end of the cycles was calculated. The cycle was repeated five times.

2.5. Photocatalytic Tests

The photocatalytic efficiency of the TP-Hy/N-TiA and the TP-Hy/P25 coatings was tested by the colorimetric method using the Techkon Spectrodens colorimeter. The photodegradation of methyl orange (MeO, 0.1 mM) and methylene blue (MB, 0.1 mM), usually used as pollutant simulants in photocatalytic experiments, was monitored under artificial solar irradiation of a 300 W Ultra Vitalux lamp (Osram, GmbH, Munich, Germany). Stained samples were placed 14 cm from the lamp: the irradiance on the samples was ~ 56 mW/cm² in the 300–800 nm range and ~ 5.5 mW/cm² in the UVA + B range, as reported in [86]. To estimate the photocatalytic discoloration of MeO and MB stains over time, the normalized chroma change ΔC^* at different exposure times t , was used:

$$\Delta C^* (\%) = \sqrt{\frac{(a^*(t) - a^*(0))^2 + (b^*(t) - b^*(0))^2}{(a_c^* - a^*(0))^2 + (b_c^* - b^*(0))^2}} \times 100 \quad (2)$$

where $a^*(t)$ and $b^*(t)$ and $a^*(0)$ and $b^*(0)$ are the CIELAB space colorimetric coordinates at time t and $t = 0$, respectively, whereas a_c^* and b_c^* are the coordinates measured on clean stones [87]. At least nine regions of a few mm² areas were examined, and the results were averaged for three samples for each case.

Two different photocatalytic experiments were performed. In one experiment, the TP-Hy/N-TiA and the TP-Hy/P25 treatments were applied directly to the *Lecce stone* with and without the paint layer, and the organic pollutants, MeO and MB, were spread by brush on the treated stone. In this way, the coating's ability to prevent degradation due to dirt deposits was tested. In the other experiment, carried out only on painted stone, the organic pollutants were spread directly on the stone, and the treatments were applied on the stains only subsequently. In this way, the cleaning capacity of the coating was assessed.

3. Results

3.1. Petrographic Analysis

Petrographic analysis by means of a transmitted light polarizing microscope displays the features of the structure and texture of *Lecce stone* (Figure 2).

Lecce stone is a fine-grained biocalcarenite, consisting mainly of micritic matrix, mixed with bioclasts and cryptocrystalline calcite cement. Chemically, it is composed of approximately 90% calcium carbonate. The insoluble fraction consists of clay minerals and glauconite [66]. Characteristic fossils such as planktonic foraminifera and calcareous nanofossils immersed in the matrix are clearly recognizable [88]. According to the Folk

classification, it can be classified as biomicrite [67]. The porosity (about 40%) is mainly due to open pores with radii between 0.5 and 4 μm [89].

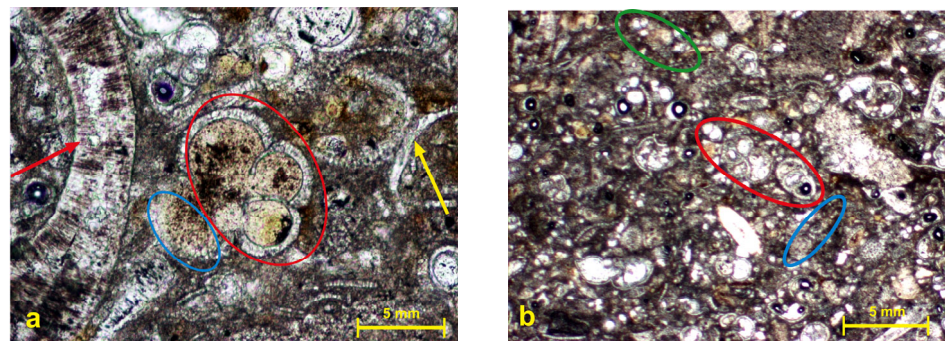


Figure 2. Polarized transmitted light optical microscope photomicrographs of *Lecce stone*. Several microfossils are recognizable: planktonic Foraminifera, Globigerina-like (e.g., red arrow and red ellipse), fragments of Bivalves (e.g., yellow arrow) and Ostracods (e.g., blue ellipse) in (a); Bivalves (e.g., green ellipse), Foraminifera (e.g., red ellipse) and Echinoderms (e.g., blue ellipse) in (b).

3.2. Raman and XRD Characterization of the Synthesized TiO_2

Raman investigations were carried out to discriminate the crystalline nature, phase purity and size of synthesized TiO_2 particles. In Figure 3a, the Raman spectrum of N-TiA powder, obtained by drying the sol, is reported: the characteristic Raman peaks of crystalline TiO_2 with an anatase structure and a small contribution of brookite (marked B in the figure) are observed. Raman spectroscopy is very sensitive to the local order of TiO_2 : the Raman peaks, as the particle size decreases, show asymmetric broadening and a large blue shift with respect to crystalline (bulk) anatase [90]. The main peak of anatase at 144 cm^{-1} is shifted to $151\text{--}155\text{ cm}^{-1}$ in N-TiA, and its width (FWHM) increases from 12 to 22 cm^{-1} . This is compatible with anatase nanocrystals in N-TiA of 5–10 nm size [91].

The XRD pattern of the TiO_2 powder, obtained by drying the synthesized nanosol at $60\text{ }^\circ\text{C}$, is shown in Figure 3b. The anatase and brookite phases in the diffractogram are clearly identified, in agreement with Raman results. The main diffraction peak of anatase (101) overlaps with the (120) and (111) reflections of brookite. The crystallite size of the N-TiA nanoparticles was determined by the line broadening of the main diffraction peak (101) of anatase by the Scherrer equation [63]: the result gives $4.5 \pm 1.0\text{ nm}$.

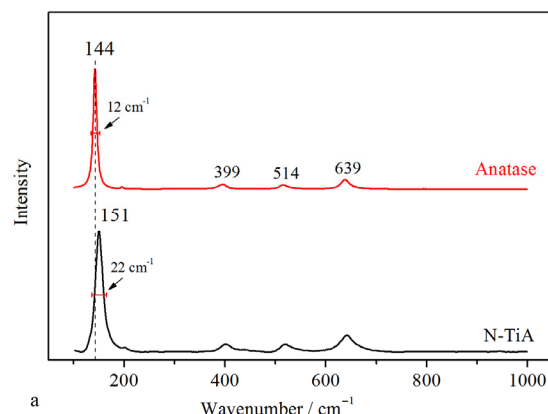


Figure 3. Cont.

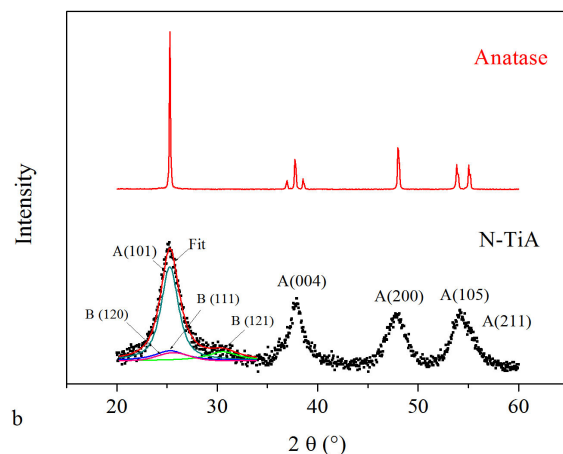


Figure 3. (a) Raman spectra of crystalline anatase and N-TiA nanopowder. The FWHM of the main peak is indicated by arrows; (b) XRD pattern of N-TiA nanopowder and crystalline anatase: (A) anatase; (B) brookite. In the N-TiA XRD, the fit (red line) to the main peak (at about 26°) is obtained by overlapping of contributions from A(101) (cyan line), B(120) (blue line), B(111) (pink line) and B(121) (green line) reflection planes.

3.3. Characterizations of the Coatings Applied on Raw Lecce stone

Ten stones were coated by brushing them with the hydrophobic TP-Hy treatment; five of these were successively coated with the photocatalytic treatment N-TiA and five with P25. The amount of one application of TP-Hy hydrophobic and three applications of photocatalytic N-TiA or P25 was calculated from the weight difference after and before the applications: $2.2 \pm 0.5 \text{ mg/cm}^2$, $0.45 \pm 0.03 \text{ mg/cm}^2$ and $0.49 \pm 0.01 \text{ mg/cm}^2$ for TP-Hy, N-TiA and P25, respectively.

SEM-EDS allowed us to investigate the surface microstructure and the elemental composition of *Lecce stone* before and after the application of the TP-Hy/N-TiA and TP-Hy/P25 coatings.

In Figure 4a, a secondary electron image of an untreated sample is reported. *Lecce stone* is an organogenic carbonate stone, quite compact and characterized by a fine-grained structure. The granular stone structure made by clasts of micrometric size and by intergranular porosity is evident. Figure 4b–e shows the SEM measurements performed on treated stones. The EDS maps of Si and Ti show that the distribution of the coating is quite homogeneous, with small and rare aggregates of TiO_2 (Figure 4c,e) for both sols.

Table 1 reports the elemental composition determined for the areas displayed in Figure 4a–c. The standards employed by the instrument are SiO_2 for Si, CaF_2 for Ca, SrTiO_3 for Ti, apatite for P and Fe_2O_3 for Fe. The program automatically converts cation concentration to oxide concentration. All concentrations are expressed in oxide wt%. The abbreviation b.d.l. stands for below detection limit (approximately 0.1% wt). Because of the less-constrained geometry in analyzing areas, the obtained concentrations have to be considered semi-quantitative and are normalized to 100% for comparison among them.

To verify that the treatments do not alter the original appearance of the stone, the total colorimetric variation ΔE^* due to the application of TP-Hy/N-TiA and TP-Hy/P25 coatings was measured on the surface of the samples before and after the treatments.

The results are summarized in Table 2, where the average colorimetric coordinates L^* , a^* , b^* taken at 27 points and the calculated ΔE^* are reported.

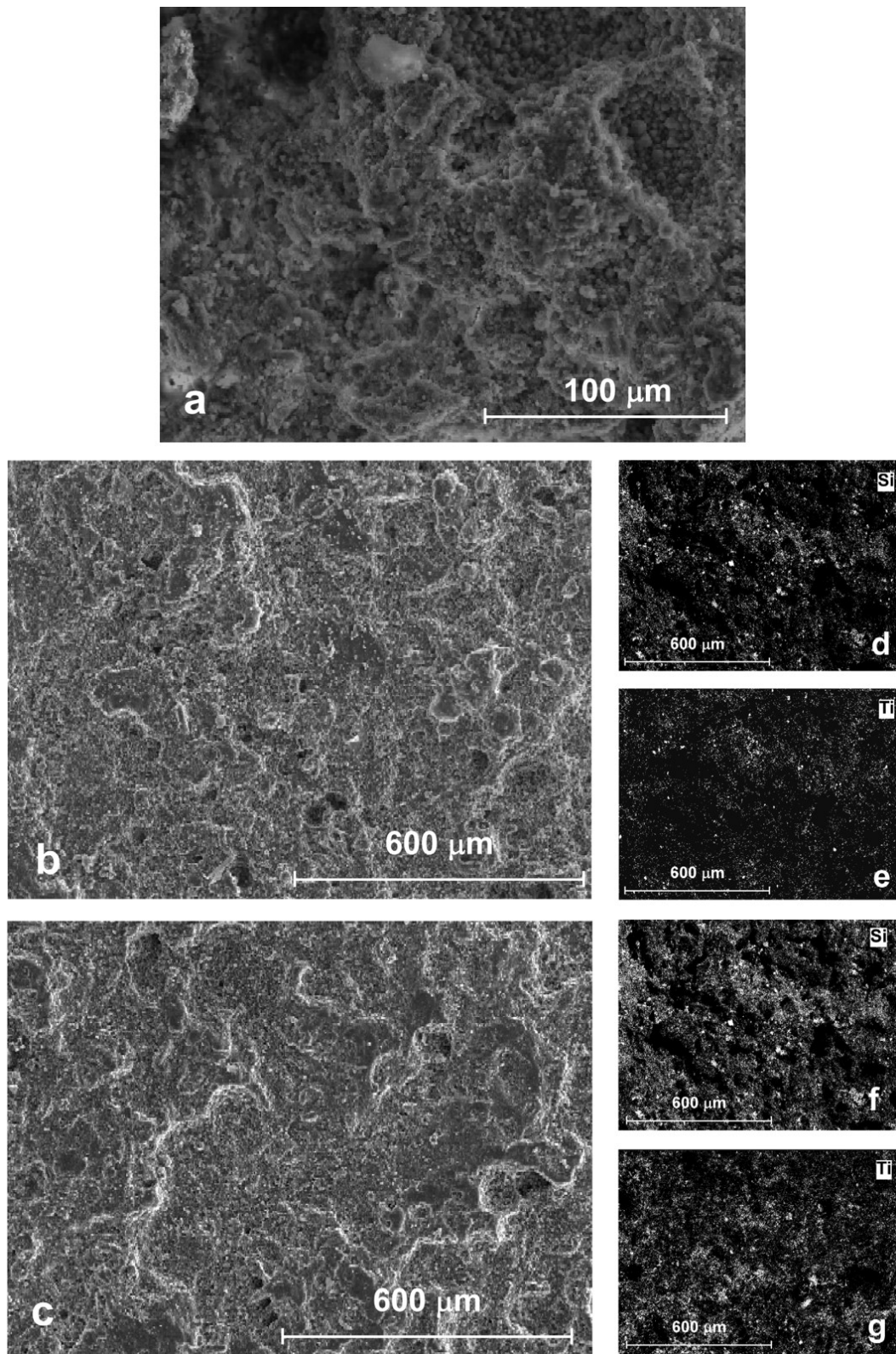


Figure 4. SEM image of untreated *Lecce stone* (a), TP-Hy/N-TiA (b) and TP-Hy/P25 (c) *Lecce stone*, Si (d,f) and Ti (e,g) EDS maps.

Table 1. Semi-quantitative composition of uncoated and coated *Lecce stone* samples obtained by EDS analysis on the areas of Figure 4. wt% = concentration of the oxide; b.d.l. = below detection limit.

Oxide	Uncoated (wt%)	TP-Hy/N-TiA (wt%)	TP-Hy/P25 (wt%)
SiO ₂	4.41	28.56	31.68
P ₂ O ₅	3.17	b.d.l.	b.d.l.
CaO	89.78	62.76	46.17
TiO ₂	b.d.l.	7.83	21.60
FeO	2.64	0.85	0.54

Table 2. Colorimetric data of coated and uncoated *Lecce stones*. In brackets is the standard deviation.

<i>Lecce stone</i>	L*	a*	b*	ΔE*
Uncoated	80.9 (5)	1.5 (4)	14.3 (7)	-
Coated TP-Hy/N-TiA	79.9 (8)	2.1 (4)	15.3 (9)	1.5 (9)
Uncoated	82.3 (6)	1.8 (3)	14.6 (5)	-
Coated TP-Hy/P25	80.6 (3)	2.5 (5)	16.7 (4)	2.8 (6)

There are no evident changes in the aesthetic appearance of the coated stone surfaces. The color difference induced by both treatments is very low and lower for N-TiA than for P25. A slight yellowing (increase in the chroma coordinate b^*) associated with a negligible decrease in luminance can be noted for the stones treated with P25. The values of the total color difference ΔE^* after the application of the TP-Hy/N-TiA and TP-Hy/P25 treatments are at the limit of the human eye perceptibility threshold, usually reported as $\Delta E^* \approx 3$ [7,92].

Capillary rising is one of the most important mechanisms for water penetration into natural or artificial building materials and is the main cause of building degradation. The influence of the coatings on the behavior of raw stones against water was investigated through measurements of water capillary absorption before and after coating. The curves of the amount of water capillary absorbed by the samples per unit area Q_i (kg/m²) at time t_i plotted as a function of the square root of time (in seconds) are shown in Figure 5. The data are averaged on five samples for each type of coating. The slope of the linear fit to the curve in Figure 5 in the first 60 min gives the absorption coefficient AC_{60} , reported in Table 3. No significant differences in the absorption behavior are observed in the coated samples.

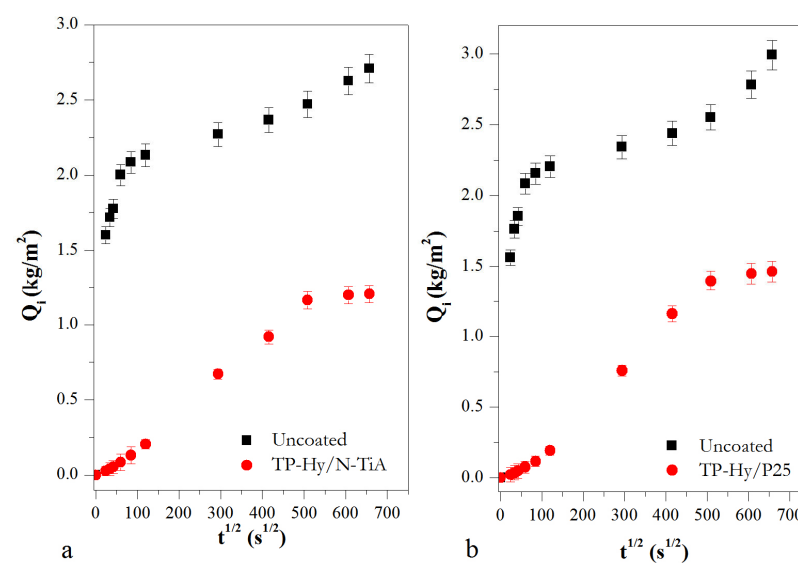
**Figure 5.** Capillarity water absorption tests carried out on *Lecce stone* before and after treatments: (a) uncoated and TP-Hy/N-TiA; (b) uncoated and TP-Hy/P25.

Table 3. Values of the absorption coefficient AC_{60} obtained by the slope of the linear fit to the curve in Figure 5 in the first 60 min. Standard deviations are in brackets.

Treatments	AC_{60} (kg/(m ² s ^{1/2})) before Coating	AC_{60} (kg/(m ² s ^{1/2})) after Coating
TP-Hy/N-TiA	0.041 (3)	0.0013 (1)
TP-Hy/P25	0.042 (1)	0.0012 (2)

As expected, the untreated *Lecce stone*, being characterized by high porosity, absorbs large amounts of water: in the first ten minutes, it reaches approximately half of the total absorbed water and continues to absorb water for the entire duration of the test (five days) without reaching a constant value. On the contrary, the two treatments show high effectiveness in reducing water absorption by capillarity. At the end of the test, the Q_i values of the coated samples are approximately 50% lower than those of the untreated stones.

Lecce stone is characterized by high permeability to water vapor. The results of the reduction of vapor permeability on coated samples are reported as the variation in the mass of water vapor through the stone as a function of time measured at the steady state. Steady state was reached in 96 h for both treated and untreated samples. The two coatings show similar behavior: the reduction in vapor permeability is significant, about 40%, for both treatments. It is not unusual that hydrophobic coatings can result in a strong reduction in water permeability when used on porous substrates [16,93].

Static contact angle (CA) measurements were carried out on uncoated and TP-Hy/N-TiA- and TP-Hy/P25-coated samples. On uncoated *Lecce stone*, due to its large porosity, the drop is immediately absorbed, making it impossible to measure the CA. On the contrary, the surface of the treated samples shows a high water-repellency, as evident from the photos of the water drops shown in Figure 6.

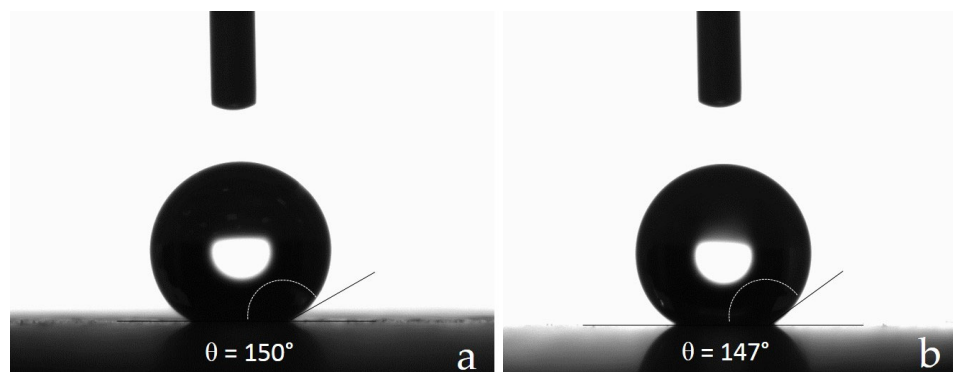


Figure 6. Water drops deposited on treated samples, TP-Hy/N-TiA (a) and TP-Hy/P25 (b), for the static contact angle measurement.

Water repellence is a desirable property of the surface to reduce water-induced degradation in natural stone. Therefore, several studies are aimed at giving stone surfaces greater hydrophobicity ($120^\circ < CA < 150^\circ$) [30–32,49,93] or, even better, super-hydrophobicity ($CA > 150^\circ$) [53,85,94].

Hydrophobic treatment is clearly very efficient in the protection of the stone by water. Both treatments show very high CA values, suggesting super hydrophobicity: for TP-Hy/N-TiA, $CA = 150 \pm 3^\circ$, and it is slightly lower in the case of the TP-Hy/P25 treatment ($CA = 147 \pm 5^\circ$).

Since rain and solar irradiation are among the main degradation agents, accelerated ageing tests were performed on untreated and treated *Lecce stone*. The hydrophobic properties of the coatings measured by means of the static contact angle at the end of each rain and artificial solar irradiation cycle do not change after ageing: the static contact angle after

the fourth ageing cycle is approximately $145 \pm 3^\circ$ for TP-Hy/N-TiA and approximately $140 \pm 3^\circ$ for TP-Hy/P25 (Figure S1).

Regarding the resistance to salt crystallization, both treatments improve the resistance of the *Lecce stone*: a decrease in mass loss after five cycles (Figure 7) from -16.6% (untreated) to -2.7% (TP-Hy/N-TiA) and -0.2% (TP-Hy/P25) is observed. As can be seen from the images in Figure 7, the uncoated *Lecce stone* is completely fractured, whereas the coated samples show superficial erosion with evident salt efflorescence. By Raman spectroscopy measurement (Figure S2), the crystallized salt is identified as thenardite.

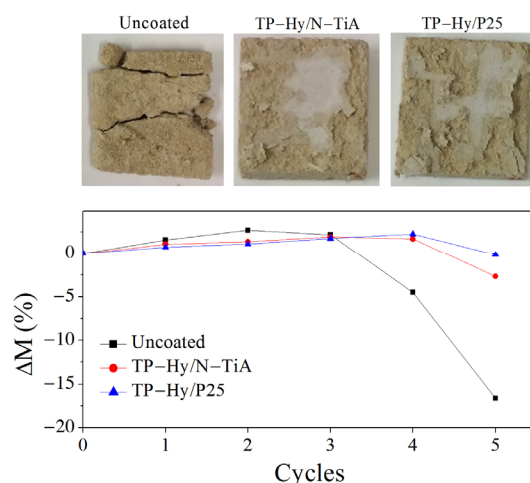


Figure 7. Photographs of the *Lecce stone* samples at the end of the salt crystallization test and mass difference (%) during the crystallization cycles.

3.4. Photocatalytic Cleaning Tests on Raw *Lecce stone*

To assess the photocatalytic efficiency of the proposed TiO_2 coatings, TP-Hy/N-TiA- and TP-Hy/P25-treated and untreated raw *Lecce stones* were stained with MeO and MB and subjected to artificial solar irradiation, as detailed in the experimental section. The colorimetric measurements were carried out at defined time intervals.

In Figure 8a,b, the normalized colorimetric variations of the chroma, as defined in Equation (2), are displayed as a function of the irradiation time. The coated *Lecce stone* samples show, for both treatments, good degradation of MeO (Figure 8a): TP-Hy/N-TiA degrades the stain mainly in the first hours of exposure, reaching about 80% stain discoloration in six hours, whereas TP-Hy/P25 shows a slightly lower efficiency, reaching in the same amount of time about 70% photodegradation.

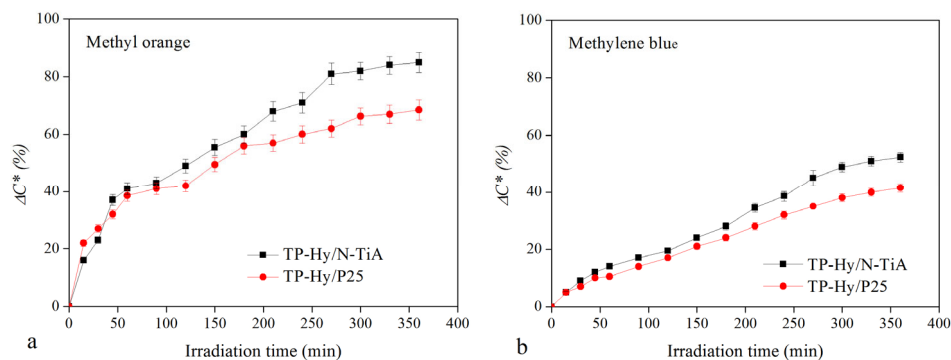


Figure 8. ΔC^* (%) of MeO-stained (a) and MB-stained (b) *Lecce stone* as a function of the irradiation time.

The photodegradation of MB (Figure 8b) is slightly lower than methyl orange. In this case too, N-TiA proved to be more efficient than P25: in the same time (360 min), N-TiA reaches more than 50% discoloration, whereas P25 reaches approximately 40%.

The photochemical degradation percentages of the Meo and MB dyes on the untreated *Lecce stone*, in the 6 h of irradiation, are about 15% and 10%, respectively.

3.5. Characterizations of the Coatings Applied on Painted *Lecce stone*

As on the raw *Lecce stone*, it has also been verified that the treatments on the painted stone do not induce chromatic alterations on the painted surfaces. The total colorimetric variation ΔE^* due to the application of the TP-Hy/N-TiA and TP-Hy/P25 coatings was measured using equation 1. The results are summarized in Table 4, where the average colorimetric coordinates L^* , a^* , b^* detected at 27 points and the calculated ΔE^* are reported. The treatments do not induce significant chromatic alterations on *Lecce stone* painted mock-ups. The color difference ΔE^* induced by the coatings is much lower than the eye's perceptibility limit: $\Delta E^* \approx 1.0$ and $\Delta E^* \approx 1.9$ for N-TiA and P25, respectively.

Table 4. Colorimetric data and static contact angle CA of the painted *Lecce stone* model samples. The standard deviation is in brackets.

Painted <i>Lecce stone</i>	L^*	a^*	b^*	ΔE^*	CA ($^\circ$)
Uncoated	85.5 (9)	4.4 (7)	5.9 (8)	-	-
Coated TP-Hy/N-TiA	84.4 (9)	4.7 (6)	6.1 (5)	1.0 (5)	147 (2)
Uncoated	85.7 (9)	3.6 (9)	5.3 (7)	-	-
Coated TP-Hy/P25	86.8 (9)	3.2 (5)	3.8 (9)	1.9 (8)	141(2)

In addition, on painted stone, the hydrophobic treatments provide high levels of protection against water. The measured static contact angles are $147 \pm 2^\circ$ and $141 \pm 2^\circ$ for TP-Hy/N-TiA and TP-Hy/P25, respectively.

3.6. Photocatalytic Cleaning Test on Painted *Lecce stone*

As explained in the experimental section, two different tests were performed.

In one of them, the cleaning capacity of the coatings was tested: the organic pollutants were spread directly on the surface of the stone, and the photocatalytic treatments (TP-Hy/N-TiA and TP-Hy/P25) were applied on the stains only subsequently. Figure 9 shows the results of the cleaning effectiveness of the treatments carried out on the painted stones up to 6 h of irradiation. TiO_2 is able to remove the pollutants deposited on the surface: in the case of MeO, the removal percentage, measured by chroma changes, is about 80% for both treatments, while ΔC^* in the case of MB is slightly lower (approximately 50%).

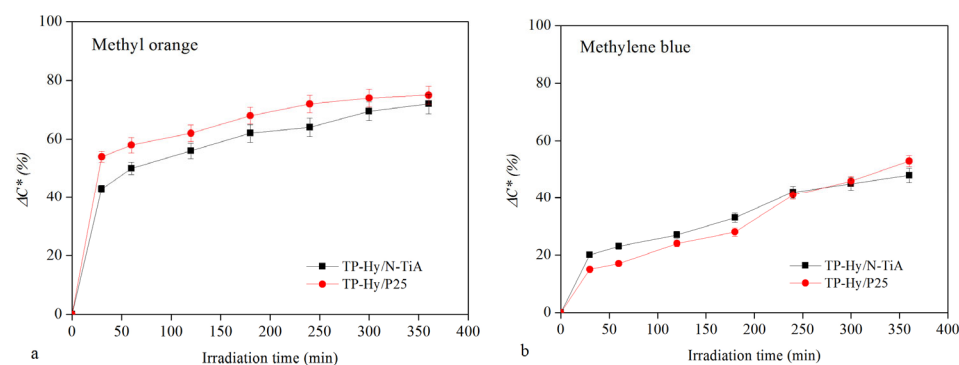


Figure 9. Cleaning treatment effectiveness on painted *Lecce stone* mock-ups. The discoloration of the MeO (a) and MB (b) stains is determined by ΔC^* (%), reported as a function of the irradiation time.

In the other experiment, self-cleaning and protective effectiveness of the coatings against a vandal attack or air pollution deposits were verified by applying the TP-Hy/N-TiA

and the TP-Hy/P25 treatments directly to the painted *Lecce stone* mock-up before staining by brush with the organic pollutants, MeO and MB.

Both treatments were able to remove the organic pollutants present on the surface (Figure 10), confirming the results obtained on the raw *Lecce stone* (see Figure 8). N-TiA proved to be very active in the photodegradation of both pollutants, comparable to or better than commercial P25: the ΔC^* measured at the end of the experiment (360 min) for N-TiA treatment is about 10–15% greater than for P25 for both MeO and MB dyes.

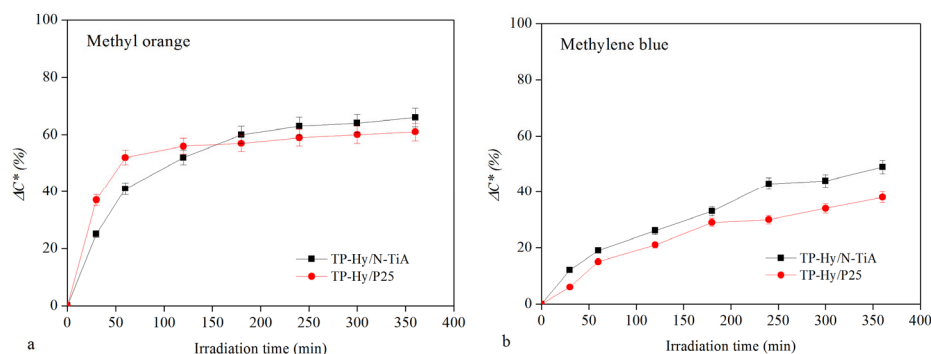


Figure 10. Self-cleaning and protective effectiveness of the coatings applied on painted *Lecce stone* mock-ups. The photodegradation of MeO (a) and MB (b), ΔC^* (%), is reported as a function of the irradiation time.

4. Conclusions

TiO₂-based nanomaterials have been widely studied in recent years as protective and self-cleaning treatments for stone artefacts. However, as far as we know, only very few authors have studied these photocatalytic coatings as cleaning methods for painted stones. In this preliminary work, we investigated the possibility of using water dispersion of TiO₂ nanoparticles and organically modified silica (OrMoSil) on painted stone for cleaning and protection purposes.

The harmlessness of the treatments was tested on raw *Lecce stone*: they did not alter the aesthetic appearance of the stone, and the water vapor permeability slightly decreased. These hydrophobic coatings are very effective in the reduction of water absorption by capillarity, by more than 50% with respect to the uncoated stone. The hydrophobic properties of the coatings measured by means of the static contact angle did not change after artificial ageing. Both treatments improved the *Lecce stone*'s resistance to salt crystallization. The self-cleaning effectiveness was verified on both raw and painted stone by staining the samples with organic dyes. The photodegradation efficiency of the synthesized TiO₂ was compared with that of the commercial P25. The results show high efficiency in the removal of stain from the stone surface coated with the TP-Hy/N-TiA treatment. The water repellence of the treatment, verified by the contact angle on both the raw and painted *Lecce stone*, is very high, slightly higher for coating with synthesized N-TiA than with commercial P25.

In addition, the TP-Hy/N-TiA treatment was effective in cleaning the painted samples without damaging their original appearance. The stains on the painted stones were removed by the cleaning treatment in 6 h simply by leaving the samples under artificial solar radiation. The synthesized N-TiA photocatalyst was found to be comparable to or better than the commercial P25.

The photocatalytic process can be proposed not only for protective and self-cleaning applications but also as an effective cleaning method for painted stones.

Supplementary Materials: The following supporting information can be downloaded at: <https://www.mdpi.com/article/10.3390/app14031261/s1>, Figure S1: Water drop deposited on treated samples TP-Hy/N-TiA (a) and TP-Hy/P25 (b) after artificial ageing, for the static contact angle measurements. Figure S2: Raman spectra of crystallized salt and thenardite standard.

Author Contributions: Conceptualization, L.B., A.C., P.P.L. and C.G.; methodology, L.B., P.P.L. and C.G.; validation, S.M., A.C., P.P.L. and C.G.; formal analysis, L.B., M.P. and S.M.; investigation, L.B., M.P. and F.S.; resources, S.M., A.C., P.P.L. and C.G.; data curation, L.B., M.P., S.M. and P.P.L.; writing—original draft preparation, L.B. and M.P.; writing—review and editing, L.B., P.P.L. and C.G.; visualization, L.B., A.C., P.P.L. and C.G.; supervision, L.B., P.P.L. and C.G. All authors have read and agreed to the published version of the manuscript.

Funding: This research was supported by NextGenerationEU—Italian Ministry of University and Research, National Recovery and Resilience Plan (NRRP); Project “Ecosystem for Sustainable Transition in Emilia-Romagna (Ecosister)”; Project code ECS00000033. Project title: Innovative cleaning proposals for the conservation of polychrome works of art.

Institutional Review Board Statement: Not applicable.

Informed Consent Statement: Not applicable.

Data Availability Statement: Data are contained within the article.

Acknowledgments: This research was supported by NextGenerationEU—Italian Ministry of University and Research, National Recovery and Resilience Plan (NRRP); Project “Ecosystem for Sustainable Transition in Emilia-Romagna (Ecosister)”; Project code ECS00000033. This work has benefited from the equipment and framework of the COMP-R Initiative, funded by the “Departments of Excellence” program of the Italian Ministry for University and Research (MUR, 2023–2027). The authors thank Andrea Comelli and Luca Barchi (Department of Chemical Science, Life and Environmental Sustainability, University of Parma) for the preparation of thin sections for microscopic investigations and Mattia Campi for experimental work during his degree thesis.

Conflicts of Interest: The authors declare no conflicts of interest.

References

1. Basso, E.; Carò, F.; Abramitis, D.H. Polychromy in Ancient Greek Sculpture: New Scientific Research on an Attic Funerary Stele at the Metropolitan Museum of Art. *Appl. Sci.* **2023**, *13*, 3102. [\[CrossRef\]](#)
2. Payne, A. Painting in Stone: Architecture and the Poetics of Marble from Antiquity to the Enlightenment, by Fabio Barry. *Art Bull.* **2022**, *104*, 160–163. [\[CrossRef\]](#)
3. Brecoulaki, H. “Precious colours” in Ancient Greek polychromy and painting: Material aspects and symbolic values. *Rev. Archéol.* **2014**, *57*, 3–35. [\[CrossRef\]](#)
4. Kreijn, L.; Ryan, G.; Rivenc, R.; Tajiri, R.V.; Chin, Z.; Wolfe, J.; Kenshe, S.; Breder, F. Conserving Outdoor Painted Sculpture. In Proceedings of the Interim Meeting of the Modern Materials and Contemporary Art Working Group of ICOM-CC, Kröller-Müller Museum, Otterlo, The Netherlands, 4–5 June 2013; The Getty Conservation Institute: Los Angeles, CA, USA, 2014; pp. 1–154.
5. Bradley, M. The importance of colour on ancient marble sculpture. *Art Hist.* **2009**, *32*, 427–457. [\[CrossRef\]](#)
6. Fassina, V. General criteria for the cleaning of stone: Theoretical aspects and methodology of application. In *Stone Material in Monuments: Diagnosis and Conservation*; Scuola Universitaria CUM Conservazione dei Monumenti: Heraklion, Crete, 1994; pp. 131–138.
7. Bellia, L.; De Natale, A.; Fragliasso, F.; Graiff, C.; Petraretti, M.; Pollio, A.; Potenza, M. Chromatic alterations induced by preservation treatments on paper: The case of Ag-functionalized nanocrystalline cellulose. *J. Cult. Herit.* **2023**, *64*, 120–131. [\[CrossRef\]](#)
8. *EN 17488:2021*; Conservation of Cultural Heritage—Procedure for the Analytical Evaluation to Select Cleaning Methods for Porous Inorganic Materials used in Cultural Heritage. European Committee for Standardization: Brussels, Belgium, 2021.
9. *EN 16581:2014*; Conservation of Cultural Heritage—Surface Protection for Porous Inorganic Materials—Laboratory Test Methods for the Evaluation of the Performance of Water Repellent Products. European Committee for Standardization: Brussels, Belgium, 2014.
10. Gomes, V.; Dionísio, A.; Pozo-Antonio, J.S. Conservation strategies against graffiti vandalism on Cultural Heritage stones: Protective coatings and cleaning methods. *Prog. Org. Coat.* **2017**, *113*, 90–109. [\[CrossRef\]](#)
11. Grossi, C.M.; Esbert, R.M.; Diaz-Pache, F.; Alonso, F.J. Soiling of building stones in urban environments. *Build. Environ.* **2003**, *38*, 147–159. [\[CrossRef\]](#)
12. Occhipinti, R.; Stroschio, A.; Belfiore, C.M.; Barone, G.; Mazzoleni, P. Chemical and colorimetric analysis for the characterization of degradation forms and surface colour modification of building stone materials. *Constr. Build. Mater.* **2021**, *302*, 124356. [\[CrossRef\]](#)
13. Douglas-Jones, R.; Hughes, J.J.; Jones, S.; Yarrow, T. Science, value and material decay in the conservation of historic environments. *J. Cult. Herit.* **2016**, *21*, 823–833. [\[CrossRef\]](#)
14. Bonazza, A.; Sabbioni, C.; Ghedini, N. Quantitative data on carbon fractions in interpretation of black crusts and soiling on European built heritage. *Atmos. Environ.* **2005**, *39*, 2607–2618. [\[CrossRef\]](#)
15. Grossi, C.M.; Brimblecombe, P. Effect of long-term changes in air pollution and climate on the decay and blackening of European stone buildings. *Geol. Soc. Spec. Publ.* **2007**, *271*, 117–130. [\[CrossRef\]](#)

16. Raneri, S.; Barone, G.; Mazzoleni, P.; Alfieri, I.; Bergamonti, L.; De Kock, T.; Cnudde, V.; Lottici, P.P.; Lorenzi, A.; Predieri, G.; et al. Efficiency assessment of hybrid coatings for natural building stones: Advanced and multi-scale laboratory investigation. *Constr. Build. Mater.* **2018**, *180*, 412–424. [[CrossRef](#)]
17. Licchelli, M.; Malagodi, M.; Weththimuni, M.L.; Zanchi, C. Water-repellent properties of fluoroelastomers on a very porous stone: Effect of the application procedure. *Prog. Org. Coat.* **2013**, *76*, 495–503. [[CrossRef](#)]
18. Vazquez-Calvo, C.; Alvarez de Buergo, M.; Fort, R.; Varas-Muriel, M.J. The measurement of surface roughness to determine the suitability of different methods for stone cleaning. *J. Geophys. Eng.* **2012**, *9*, S108–S117. [[CrossRef](#)]
19. Valentini, F.; Diamanti, A.; Carbone, M.; Bauer, E.M.; Palleschi, G. New cleaning strategies based on carbon nanomaterials applied to the deteriorated marble surfaces: A comparative study with enzyme based treatments. *Appl. Surf. Sci.* **2012**, *258*, 5965–5980. [[CrossRef](#)]
20. Vergès-Belmin, V.; Wiedemann, G.; Weber, L.; Cooper, M.; Crump, D.; Gouverne, R. A review of health hazards linked to the use of lasers for stone cleaning. *J. Cul. Herit.* **2003**, *4*, 33–37. [[CrossRef](#)]
21. Werner, M. Research on cleaning methods applied to historical stone monuments. In *Science, Technology, and European Cultural Heritage*; Baer, N.S., Sabbioni, S., Sors, A.I., Eds.; Butterworth-Heinemann: Boston, MA, USA, 1991; pp. 688–691.
22. Doehne, E.; Price, C.A. *Stone Conservation: An Overview of Current Research*, 2nd ed.; Getty Conservation Institute: Los Angeles, CA, USA, 2010; pp. 1–175. ISBN 978-1-60606-046-9.
23. Raneri, S.; Crezzini, J.; Arrighi, S.; Boschin, F.; Alfieri, I.; Barone, G.; Bergamonti, L.; Giamello, M.; Lottici, P.P.; Mazzoleni, P. Measuring weathering and nanoparticle coating impact on surface roughness of natural stones. *Stud. Conserv.* **2019**, *64*, 298–309. [[CrossRef](#)]
24. Bergamonti, L.; Graiff, C.; Simeti, S.; Casoli, A. The 20th Century Wall Paintings in the Chapel of the Fallen in Parma Cathedral (Italy): Scientific Investigations for a Correct Conservation. *Project. Appl. Sci.* **2023**, *13*, 7235. [[CrossRef](#)]
25. Magrini, D.; Bracci, S.; Cantisani, E.; Conti, C.; Rava, A.; Sansonetti, A.; Shank, W.; Colombini, M.P. A multi-analytical approach for the characterization of wall painting materials on contemporary buildings. *Spectrochim. Acta A* **2017**, *173*, 39–45. [[CrossRef](#)]
26. Amadori, M.L.; Vagnini, M.; Vivani, R.; Anselmi, C.; Chaverdi, A.A.; Callieri, P.; Marin, E.; Mengacci, V. Advances in characterization of colourful residues unearthed in Persepolis West craft zone using microscopic and spectroscopic techniques. *Microchem. J.* **2021**, *167*, 106304. [[CrossRef](#)]
27. Laureti, S.; Colantonio, C.; Burrascano, P.; Melis, M.; Calabrò, G.; Malekmohammadi, H.; Sfarra, S.; Ricci, M.; Pelosi, C. Development of integrated innovative techniques for paintings examination: The case studies of The Resurrection of Christ attributed to Andrea Mantegna and the Crucifixion of Viterbo attributed to Michelangelo’s workshop. *J. Cult. Herit.* **2019**, *40*, 1–16. [[CrossRef](#)]
28. Colantonio, C.; Lanteri, L.; Bocci, R.; Valentini, V.; Pelosi, C. “A Woman Clothed with the Sun”: The Diagnostic Study and Testing of Enzyme-Based Green Products for the Restoration of an Early 17th Century Wall Painting in the Palazzo Gallo in Bagnaia (Italy). *Appl. Sci.* **2023**, *13*, 12884. [[CrossRef](#)]
29. Pedna, A.; Pinho, L.; Frediani, P.; Mosquera, M.J. Obtaining SiO₂-fluorinated PLA bionanocomposites with application as reversible and highly-hydrophobic coatings of buildings. *Prog. Org. Coat.* **2016**, *90*, 91–100. [[CrossRef](#)]
30. Kapridaki, C.; Maravelaki-Kalaitzaki, P. TiO₂-SiO₂-PDMS nano-composite hydrophobic coating with self-cleaning properties for marble protection. *Prog. Org. Coat.* **2013**, *76*, 400–410. [[CrossRef](#)]
31. Mosquera, M.J.; Pinho, L.; Facio, D.S.; Elhaddad, F. New nanomaterials for conservation of cultural heritage: Consolidants, hydrophobic and self-cleaning products. In *Science, Technology and Cultural Heritage, Proceedings of the 2nd International Congress on Science and Technology for the Conservation of Cultural Heritage, Sevilla, Spain, 24–27 June 2014*; CRC Press: Boca Raton, FL, USA, 2014; pp. 121–126.
32. Kapridaki, C.; Pinho, L.; Mosquera, M.J.; Maravelaki-Kalaitzaki, P. Producing photoactive, transparent and hydrophobic SiO₂-crystalline TiO₂ nanocomposites at ambient conditions with application as self-cleaning coatings. *Appl. Catal. B* **2014**, *156*, 416–427. [[CrossRef](#)]
33. Sansonetti, A.; Bertasa, M.; Canevali, C.; Rabbolini, A.; Anzani, M.; Scalarone, D. A review in using agar gels for cleaning art surfaces. *J. Cult. Herit.* **2020**, *44*, 285–296. [[CrossRef](#)]
34. Cremonesi, P.; Casoli, A. Enzymes as tools for conservation of works of art. *J. Cult. Herit.* **2021**, *50*, 73–87. [[CrossRef](#)]
35. Ortega-Morales, B.O.; Gaylarde, C.C. Bioconservation of historic stone buildings—An updated review. *Appl. Sci.* **2021**, *11*, 5695. [[CrossRef](#)]
36. Baglioni, P.; Chelazzi, D.; Giorgi, R. Cleaning of wall paintings and stones. In *Nanotechnologies in the Conservation of Cultural Heritage*; Springer: Dordrecht, The Netherlands, 2015; pp. 61–82. [[CrossRef](#)]
37. Siano, S.; Agresti, J.; Cacciari, I.; Ciofini, D.; Mascalchi, M.; Osticioli, I.; Mencaglia, A.A. Laser cleaning in conservation of stone, metal, and painted artifacts: State of the art and new insights on the use of the Nd: YAG lasers. *Appl. Phys. A* **2012**, *106*, 419–446. [[CrossRef](#)]
38. Balliana, E.; Ricci, G.; Pesce, C.; Zendri, E. Assessing the value of green conservation for cultural heritage: Positive and critical aspects of already available methodologies. *Int. J. Conserv. Sci.* **2016**, *7*, 185–202.
39. Franzoni, E.; Volpi, L.; Bonoli, A.; Spinelli, R.; Gabrielli, R. The environmental impact of cleaning materials and technologies in heritage buildings conservation. *Energy Build.* **2018**, *165*, 92–105. [[CrossRef](#)]
40. Di Turo, F.; Medeghini, L. How green possibilities can help in a future sustainable conservation of cultural heritage in Europe. *Sustainability* **2021**, *13*, 3609. [[CrossRef](#)]
41. Pasquale, S.; Zimbone, M.; Ruffino, F.; Stella, G.; Gueli, A.M. Evaluation of the Photocatalytic Activity of Water-Based TiO₂ Nanoparticle Dispersions Applied on Historical Painting Surfaces. *Heritage* **2021**, *4*, 1854–1867. [[CrossRef](#)]

42. Baglioni, M.; Giorgi, R.; Berti, D.; Baglioni, P. Smart cleaning of cultural heritage: A new challenge for soft nanoscience. *Nanoscale* **2012**, *4*, 42–53. [[CrossRef](#)]
43. David, M.E.; Ion, R.M.; Grigorescu, R.M.; Iancu, L.; Andrei, E.R. Nanomaterials used in conservation and restoration of cultural heritage: An up-to-date overview. *Materials* **2020**, *13*, 2064. [[CrossRef](#)]
44. Serafini, I.; Ciccola, A. Nanotechnologies and nanomaterials: An overview for cultural heritage. In *Nanotechnologies and Nanomaterials for Diagnostic, Conservation and Restoration of Cultural Heritage*; Lazzara, G., Fakhrulli, R.F., Eds.; Elsevier: Amsterdam, The Netherlands, 2018; pp. 325–380. [[CrossRef](#)]
45. Bosch-Roig, P.; Lustrato, G.; Zanardini, E.; Ranalli, G. Biocleaning of Cultural Heritage stone surfaces and frescoes: Which delivery system can be the most appropriate? *Ann. Microbiol.* **2015**, *65*, 1227–1241. [[CrossRef](#)]
46. Peterka, F. Novel Light Cleaning Technology for Cultural Heritage Protection. In *Handbook of Cultural Heritage Analysis*; D'Amico, S., Venuti, V., Eds.; Springer: Cham, Switzerland, 2022; pp. 1051–1073. [[CrossRef](#)]
47. Pasquale, S.; Privitera, V.; Miritello, M.; Zimbone, M.; Politi, G.; Gueli, A.M. Application of a new photocatalytic nanomaterial obtained by Pulse Laser Ablation for Polychrome Paintings Conservation: A feasibility study. *Estud. Conserv. Restauro.* **2019**, *10*, 31–43.
48. Pasquale, S.; Politi, G.; Pronti, L.; Romani, M.; Viviani, G.; Guidi, M.C.; Gueli, A.M. Analysis of the distribution of titanium oxide nanoparticles on paintings. *J. Phys. Conf. Ser.* **2022**, *2204*, 012070. [[CrossRef](#)]
49. Gherardi, F.; Roveri, M.; Goidanich, S.; Toniolo, L. Photocatalytic nanocomposites for the protection of European architectural heritage. *Materials* **2018**, *11*, 65. [[CrossRef](#)]
50. Franzoni, E.; Fregni, A.; Gabrielli, R.; Graziani, G.; Sassoni, E. Compatibility of photocatalytic TiO₂-based finishing for renders in architectural restoration: A preliminary study. *Build. Environ.* **2014**, *80*, 125–135. [[CrossRef](#)]
51. Colangiuli, D.; Calia, A.; Bianco, N. Novel multifunctional coatings with photocatalytic and hydrophobic properties for the preservation of the stone building heritage. *Constr. Build. Mater.* **2015**, *93*, 189–196. [[CrossRef](#)]
52. Wei, Y.; Wu, Q.; Meng, H.; Zhang, Y.; Cao, C. Recent advances in photocatalytic self-cleaning performances of TiO₂-based building materials. *RSC Adv.* **2023**, *13*, 20584–20597. [[CrossRef](#)] [[PubMed](#)]
53. Cannistraro, G.; Cannistraro, M.; Piccolo, A.; Restivo, R. Potentials and limits of oxidative photocatalysis and possible applications in the field of cultural heritage. *Adv. Mat. Res.* **2013**, *787*, 111–117. [[CrossRef](#)]
54. Ruffolo, S.A.; La Russa, M.F. Nanoparticles in the Field of Built Heritage Restoration: Challenges and Limits. In *Handbook of Cultural Heritage Analysis*; D'Amico, S., Venuti, V., Eds.; Springer International Publishing: Cham, Switzerland, 2022; pp. 1033–1050. ISBN 9783030600167. [[CrossRef](#)]
55. Zarzuela, R.; Luna, M.; Carrascosa, L.A.; Mosquera, M.J. Preserving cultural heritage stone: Innovative consolidant, superhydrophobic, self-cleaning, and biocidal products. In *Advanced Materials for the Conservation of Stone*; Hosseini, M., Karapanagiotis, I., Eds.; Springer: Cham, Switzerland, 2018; pp. 259–275. [[CrossRef](#)]
56. Coutinho, C.A.; Gupta, V.K.J. Photocatalytic degradation of methyl orange using polymer–titania microcomposites. *Colloid. Interface Sci.* **2009**, *333*, 457–464. [[CrossRef](#)] [[PubMed](#)]
57. Chen, H.; Nanayakkara, C.E.; Grassian, V.H. Titanium Dioxide Photocatalysis in Atmospheric Chemistry. *Chem. Rev.* **2012**, *112*, 5919–5948. [[CrossRef](#)] [[PubMed](#)]
58. Mohammed, S.S.; Shnain, Z.Y.; Abid, M.F. Use of TiO₂ in photocatalysis for air purification and wastewater treatment: A review. *Eng. Technol. J.* **2022**, *40*, 1131–1143. [[CrossRef](#)]
59. Chen, D.; Cheng, Y.; Zhou, N.; Chen, P.; Wang, Y.; Li, K.; Huo, S.; Cheng, P.; Peng, P.; Zhang, R.; et al. Photocatalytic degradation of organic pollutants using TiO₂-based photocatalysts: A review. *J. Clean. Pro.* **2020**, *268*, 121725. [[CrossRef](#)]
60. Al-Mamun, M.R.; Kader, S.; Islam, M.S.; Khan, M.Z.H. Photocatalytic activity improvement and application of UV-TiO₂ photocatalysis in textile wastewater treatment: A review. *J. Environ. Chem. Eng.* **2019**, *7*, 103248. [[CrossRef](#)]
61. Kumar, S.; Sharma, R.; Gupta, A.; Dubey, K.; Khan, A.M.; Singhal, R.; Kumar, R.; Bharti, A.; Singh, P.; Kant, R.; et al. TiO₂ based Photocatalysis membranes: An efficient strategy for pharmaceutical mineralization. *Sci. Total Environ.* **2022**, *845*, 157221. [[CrossRef](#)]
62. Bergamonti, L.; Graiff, C.; Bergonzi, C.; Potenza, M.; Reverberi, C.; Ossiprandi, M.C.; Lottici, P.P.; Bettini, R.; Elviri, L. Photodegradation of Pharmaceutical Pollutants: New Photocatalytic Systems Based on 3D Printed Scaffold-Supported Ag/TiO₂ Nanocomposite. *Catalysts* **2022**, *12*, 580. [[CrossRef](#)]
63. Fornasini, L.; Bergamonti, L.; Bondioli, F.; Bersani, D.; Lazzarini, L.; Paz, Y.; Lottici, P.P. Photocatalytic N-doped TiO₂ for self-cleaning of limestones. *Eur. Phys. J. Plus* **2019**, *134*, 539. [[CrossRef](#)]
64. Pinho, L.; Elhaddad, F.; Facio, D.S.; Mosquera, M.J. A novel TiO₂-SiO₂ nanocomposite converts a very friable stone into a self-cleaning building material. *Appl. Surf. Sci.* **2013**, *275*, 389–396. [[CrossRef](#)]
65. Khannyra, S.; Luna, M.; Gil, M.A.; Addou, M.; Mosquera, M.J. Self-cleaning durability assessment of TiO₂/SiO₂ photocatalysts coated concrete: Effect of indoor and outdoor conditions on the photocatalytic activity. *Build. Environ.* **2022**, *211*, 108743. [[CrossRef](#)]
66. Luna, M.; Mosquera, M.J.; Vidal, H.; Gatica, J.M. Au-TiO₂/SiO₂ photocatalysts for building materials: Self-cleaning and de-polluting performance. *Build. Environ.* **2019**, *164*, 106347. [[CrossRef](#)]
67. Folk, R.L. Spectral subdivision of limestone types. In *Classification of Carbonate Rocks—A Symposium*; Ham, W.E., Ed.; American Association of Petroleum Geologists Mem: Tulsa, OK, USA, 1962; pp. 62–84.
68. Ghio, F.; Stefanelli, E.M.; Ampolo, E. The Flight of Saint Mary Magdalene—A Case Study of the Dismantling, Repositioning and Restoration of a Votive Aedicule and Wall Painting in Nardò, Lecce, Italy. *Heritage* **2023**, *6*, 3429–3447. [[CrossRef](#)]

69. Esposito, D.; Vitarelli, F.; Vita, L.; D'Onofrio, M. Conoscenza e progetto. Un caso di studio. Santa Maria di Cerrate. In *RPR, Rilievo, Progetto, Riuso*; Maggioli: Santarcangelo di Romagna, Italy, 2017; pp. 285–298. ISBN 9788891624833.
70. De Pascalis, D.G.; Leucci, G.; De Giorgi, L.; Giuri, F.; Scardozi, G. The Basilica of Santa Caterina d'Alessandria in Galatina (Lecce, Italy): NDT surveys for the conservation project. In Proceedings of the 2019 IMEKO TC-4 International Conference on Metrology for Archaeology and Cultural Heritage, Florence, Italy, 4–6 December 2019; pp. 369–371, ISBN 978-92-990084-5-4.
71. Gryparis, C.; Krasoudaki, T.; Maravelaki, P.N. Self-Cleaning Coatings for the Protection of Cementitious Materials: The Effect of Carbon Dot Content on the Enhancement of Catalytic Activity of TiO₂. *Coatings* **2022**, *12*, 587. [\[CrossRef\]](#)
72. Zhu, H.; Jiang, R.; Fu, Y.; Guan, Y.; Yao, J.; Xiao, L.; Zeng, G. Effective photocatalytic decolorization of methyl orange utilizing TiO₂/ZnO/chitosan nanocomposite films under simulated solar irradiation. *Desalination* **2012**, *286*, 41–48. [\[CrossRef\]](#)
73. Nguyen, C.H.; Fu, C.C.; Juang, R.S. Degradation of methylene blue and methyl orange by palladium-doped TiO₂ photocatalysis for water reuse: Efficiency and degradation pathways. *J. Clean. Prod.* **2018**, *202*, 413–427. [\[CrossRef\]](#)
74. Bouarioua, A.; Zerdaoui, M. Photocatalytic activities of TiO₂ layers immobilized on glass substrates by dip-coating technique toward the decolorization of methyl orange as a model organic pollutant. *J. Environ. Chem. Eng.* **2017**, *5*, 1565–1574. [\[CrossRef\]](#)
75. Edwards, H.G.M.; Vandenabeele, P.; Colomban, P. From Frescoes to Paintings. In *Raman Spectroscopy in Cultural Heritage Preservation*; Cultural Heritage Science; Springer: Cham, Switzerland, 2023; pp. 169–214. [\[CrossRef\]](#)
76. Mastrotheodoros, G.P.; Beltsios, K.G. Pigments—Iron-based red, yellow, and brown ochres. *Archaeol. Anthropol. Sci.* **2022**, *14*, 35. [\[CrossRef\]](#)
77. *UNI 10921:2001*; Conservation of Cultural Property—Test Methods—Natural and Artificial Stone Materials—Hydrophobic Products. UNI Ente Nazionale Italiano di Unificazione: Milan, Italy, 2001.
78. Baiza, B.; Gil, M.; Galacho, C.; Candeias, A.; Girginova, P.I. Preliminary Studies of the Effects of Nanoconsolidants on Mural Paint Layers with a Lack of Cohesion. *Heritage* **2021**, *4*, 3288–3306. [\[CrossRef\]](#)
79. Regazzoni, L.; Cavallo, G.; Biondelli, D.; Gilardi, J. Microscopic analysis of wall painting techniques: Laboratory replicas and romanesque case studies in Southern Switzerland. *Stud. Conserv.* **2018**, *63*, 326–341. [\[CrossRef\]](#)
80. *UNI EN 15886:2010*; Conservation of Cultural Property—Test Methods—Color Measurement of Surfaces. UNI Ente Nazionale Italiano di Unificazione: Milan, Italy, 2010.
81. *UNI EN 15801:2010*; Conservation of Cultural Property—Test Methods—Determination of Water Absorption by Capillarity. UNI Ente Nazionale Italiano di Unificazione: Milan, Italy, 2010.
82. Washburn, E.W. The dynamics of capillary flow. *Phys. Rev.* **1921**, *17*, 273–283. [\[CrossRef\]](#)
83. Manoudis, P.N.; Karapanagiotis, I.; Tsakalof, A.; Zuburtikudis, I.; Kolinkeová, B.; Panayiotou, C. Superhydrophobic films for the protection of outdoor cultural heritage assets. *Appl. Phys. A* **2009**, *97*, 351–360. [\[CrossRef\]](#)
84. *UNI EN 15802: 2010*; Conservation of Cultural Property—Test Methods—Determination of Static Contact Angle. UNI Ente Nazionale Italiano di Unificazione: Milan, Italy, 2010.
85. Bergamonti, L.; Bondioli, F.; Alfieri, I.; Alinovi, S.; Lorenzi, A.; Predieri, G.; Lottici, P.P. Weathering resistance of PMMA/SiO₂/ZrO₂ hybrid coatings for sandstone conservation. *Polym. Degrad. Stab.* **2018**, *147*, 274–283. [\[CrossRef\]](#)
86. *UNI EN 12370:2001*; Conservation of Cultural Property—Natural Stone Test Method—Determination of Resistance to Salt Crystallization. UNI Ente Nazionale Italiano di Unificazione: Milan, Italy, 2001.
87. Ohta, N.; Robertson, A.R. Measurement and Calculation of Colorimetric Values. In *Colorimetry: Fundamentals and Applications*; John Wiley & Sons, Ltd.: Hoboken, NJ, USA, 2005; Chapter 5; pp. 153–173.
88. Mazzei, R.; Margiotta, S.; Foresi, L.M.; Riforgiato, F.; Salvatorini, G. Biostratigraphy and chronostratigraphy of the Miocene Pietra Leccese in the type area of Lecce (Apulia, southern Italy). *Boll. Soc. Paleontol. Ital.* **2009**, *48*, 129–145.
89. Vasanelli, E.; Sileo, M.; Calia, A.; Aiello, M.A. Non-destructive techniques to assess mechanical and physical properties of soft calcarenitic stones. *Procedia Chem.* **2013**, *8*, 35–44. [\[CrossRef\]](#)
90. Sahoo, S.; Arora, A.K.; Sridharan, V. Raman line shapes of optical phonons of different symmetries in anatase TiO₂ nanocrystals. *J. Phys. Chem. C* **2009**, *113*, 16927–16933. [\[CrossRef\]](#)
91. Bersani, D.; Lottici, P.P.; Ding, X.-Z. Phonon confinement effects in the Raman scattering by TiO₂ nanocrystals. *Appl. Phys. Lett.* **1998**, *72*, 73. [\[CrossRef\]](#)
92. Mahy, M.; Van Eycken, L.; Oosterlinck, A. Evaluation of uniform color spaces developed after the adoption of CIELAB and CIELUV. *Color. Res. Appl.* **1994**, *19*, 105–121. [\[CrossRef\]](#)
93. Pinho, L.; Mosquera, M.J. Titania-silica nanocomposite photocatalysts with application in stone self-cleaning. *J. Phys. Chem. C* **2011**, *115*, 22851–22862. [\[CrossRef\]](#)
94. Karapanagiotis, I.; Pavlou, A.; Manoudis, P.N.; Aifantis, K.E. Water repellent ORMOSIL films for the protection of stone and other materials. *Mater. Lett.* **2014**, *131*, 276–279. [\[CrossRef\]](#)

Disclaimer/Publisher's Note: The statements, opinions and data contained in all publications are solely those of the individual author(s) and contributor(s) and not of MDPI and/or the editor(s). MDPI and/or the editor(s) disclaim responsibility for any injury to people or property resulting from any ideas, methods, instructions or products referred to in the content.